Journal of Materials Science Research; Vol. 2, No. 2; 2013
ISSN 1927-0585 E-ISSN 1927-0593
Published by Canadian Center of Science and Education

Effect of Heat Treatment on Strain Life of Aluminum Alloy AA 6061

Adnan N. Abood[1], Ali H. Saleh[2] & Zainab W. Abdullah[1]

[1] Technical College/Baghdad, Baghdad, Iraq

[2] Institute of Technology, Baghdad, Iraq

Correspondence: Zainab W. Abdullah, Technical College/Baghdad, Baghdad, Iraq. Tel: 964-770-296-9532. E-mail: zainab.wa83@yahoo.com

Received: September 22, 2012 Accepted: October 30, 2012 Online Published: January 30, 2013

doi:10.5539/jmsr.v2n2p51 URL: http://dx.doi.org/10.5539/jmsr.v2n2p51

Abstract

The present work encompasses the investigation of Low Cycle Fatigue (LCF) of aluminum alloy AA6061 in three conditions, annealing (O), T4 and T651. AA6061-O has the higher value of transition fatigue life (N_T) because it has the highest ductility, while the fatigue strength exponent and fatigue ductility exponent are within the range of metallic materials. The SEM morphology for specimens at strain closer to true tensile stress show multi-crack origins with secondary cracks and large final fracture zone. The striations are very clear for O-condition.

Keywords: low cycle fatigue, aluminum alloy AA6061, annealing (O), T4 and T651-conditions

1. Introduction

Aluminum and its alloys are being used successfully in a wide range of applications, from packaging to aerospace industries. Due to their good mechanical properties and low densities, these alloys have an edge over other conventional structural materials (Mustapha, Abdelhamid, & Mohamed, 2009). Age hardened aluminum alloys are of great technological importance. In particular for ground transport systems, when relatively high strength, good corrosion resistance and high toughness are required in conjunction with good formability and weldability, aluminum alloys with Mg and Si as alloying elements are used. One of the essential goals in the fatigue process study is the prediction of the fatigue life of a structure or machine component subjected to a given stress-time history. To allow this prediction, complete information about the response and behavior of the material subjected to cyclic loading is necessary (Haji, 2010; Kwon, Song, Shin, & Kwun, 2010). Borrego, Abreu, Costa and Ferreira (2004) studied low-cycle fatigue of two AlMgSi aluminum alloys AA6082-T6 and AA6060-T6 alloys. They were concluded that AA6060-T6 exhibits nearly ideal Masing behavior, while alloy AA6082-T6 presents significant deviations from the Masing model. Xiaoshan, Guoqiu , Xiangqun , Defeng and Weihua (2009) were found The deformation of the alloy and the morphology of the dislocation substructures determine the fatigue behavior of AA6063 alloy under the same equivalent stress amplitude loading when studied the fatigue behavior under several nonproportional path loadings, which were circle, ellipse, rectangle and square paths. Fatemi, Plaseieda, Khosrovanehb and Tanner (2005) were shown that the bi-linear S–N model provides a much better representation of the data than the commonly used linear model for AA6063, AA6260 and AA6082. Torsional deformation and fatigue behavior of both solid and thin-walled tubular specimens made from as-received and heat treated 6061 aluminum alloy were studied (Marini & Ismail, 2011) and, it is conclude that the S-N curve shows that heat treated T6 alloy exhibit higher fatigue life and fatigue strength compared to the as-received alloy. Santana, Gonzalez, Mesmacque and Amrouche (2009), were investigated the dynamic response of fatigue damaged 6061-T6 aluminum alloy and AISI 4140T steel specimens under high cycle fatigue and low cycle fatigue. The analysis results show an increase in the ductility of the aluminum alloy when increasing the fatigue damage level. While Ding, Hartmann, Biermann and Mughrabi (2002) studied the fatigue behavior of AA6061 as a composite materials. A low-cycle fatigue life prediction model for particulate-reinforced metal-matrix composites (MMCs) is presented. The empirical Coffin-Manson relationship is derived and the model naturally predicts that in strain-controlled low-cycle fatigue tests the MMCs with the higher volume fraction of reinforcement particles exhibit shorter fatigue lives than composites with a smaller volume fraction. Also a low cycle fatigue model has been developed to predict the fatigue life of both the unreinforced aluminum alloy and the short fibre reinforced aluminum alloy metal-matrix composites based solely on crack propagation from microstructural features (Ding, Biermann, & Hartmann, 2002). The empirical

Coffin-Manson and Basquin laws have been derived theoretically and applied to compare with total-strain controlled low-cycle fatigue life data obtained on the unreinforced 6061 aluminum alloy at 25 ^{o}C and on the aluminum alloy AA6061 matrix reinforced with Al_2O_3 short-fibres of a volume fraction of 20 vol.% and test temperatures from 100 to 150 ^{o}C. It is remarkable that the addition of high-strength Al_2O_3 fibres in the 6061 aluminum alloy matrix will not only strengthen the microstructure of the 6061 aluminum alloy, but also channel deformation at the tip of a crack into the matrix regions between the fibres and therefore constrain the plastic deformation in the matrix. The objective of this paper is to study the effect of heat treatment on strain life of AA 6061 and its microstructure variation.

2. Materials and Experimental Procedures

The material used in this study is the aluminum alloy 6061 in three tempered situations, T651 solution heat-treated and artificially aged then cold worked, T4 Solution heat treated and naturally aged to a substantially stable condition and O-annealed. The chemical composition of the material is given in Table 1.

Table 1. Chemical composition of aluminum alloy AA 6061

	%Si	%Fe	%Cu	%Mn	%Mg	%Zn	%Cr	%Al
Nominal chemical composition AA 6061	0.4-0.8	0.7 max	0.15-0.4	0.15 max	0.8-1.2	0.25 max	0.04-0.35	Balance
Aluminum alloy AA 6061	0.5793	0.106	0.211	0.0005	0.801	0.005	0.114	Balance

A tensile test was done according to ASTM B557-84. Average value of 5 specimens for each heat treatment condition was taken (Figure 1).

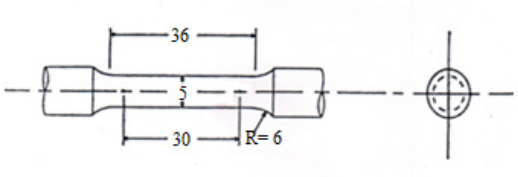

Figure 1. Tensile test specimen (All dimensions in mm)

Low-cycle fatigue tests were carried out according to ASTM 606-80. The apparatus used is of cantilever fatigue testing machine, with specimens were shown in Figure 2. This is a pure reversed bending stress with mean stress equal to zero. The surface roughness measurement showed that specimen's surface roughness was about 0.17 µm. Each fatigue curve plotted was constructed of about 10 point, each one of these points was the average value of 3 specimens. SEM examination was done to the fractured surface.

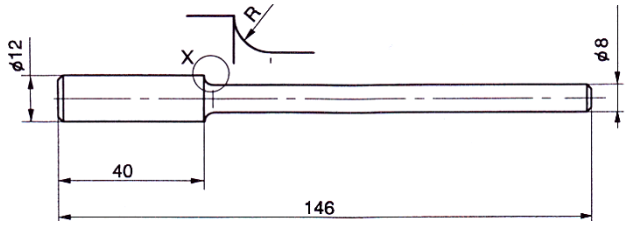

Figure 2. Fatigue test specimen (All dimensions in mm)

3. Results and Discussion

The tensile test results are present in Table 2. The tensile properties of annealing (O) condition were greatly variance as compared with T651 and T4 conditions as shown in stress-strain curve in Figures 3-5. So that, the σ_u/σ_y ratio of annealing condition is the highest value (1.7) which give an advanced indication to the cyclic hardening behavior under LCF. While the same ratio for the two other conditions have values smaller than 1.2 which gives an indication to the cyclic softening behavior under LCF (Xue, 2004).

Table 2. Mechanical properties of AA6061

		Engineering tensile strength (MPa)	Engineering yield strength (MPa)	σ_u/σ_y	Elongation %
AA 6061-T651	Nominal	310	276	---	12-17
	Experimental	338	300	1.12	13
AA 6061-T4	Nominal	241	145	---	18-23
	Experimental	307	262	1.17	19
A A6061-O	Nominal	124	55	---	25-30
	Experimental	127	73	1.7	28

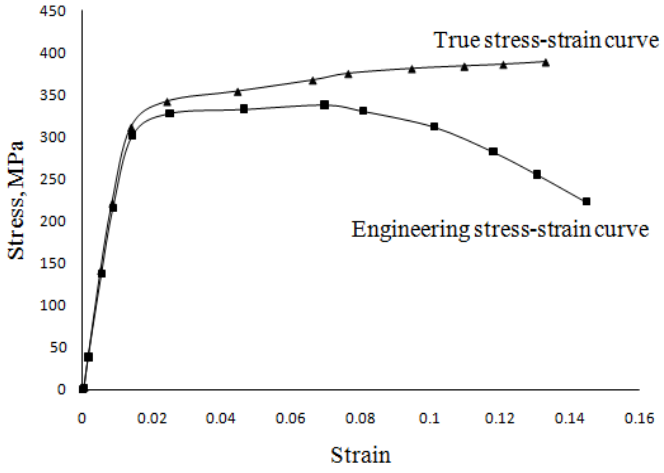

Figure 3. Engineering and true stress-strain curve for AA 6061-T651

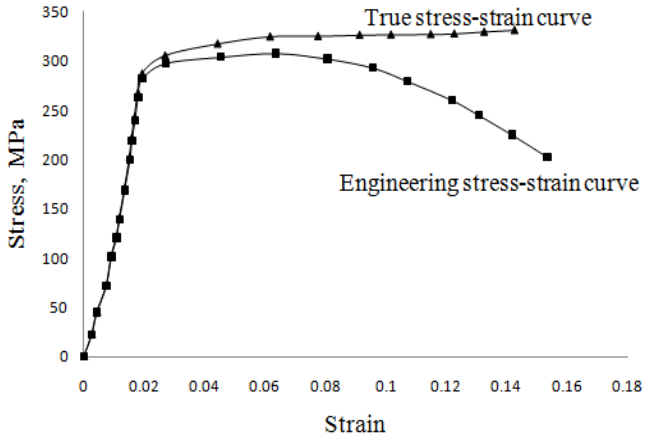

Figure 4. Engineering and true stress-strain curve for AA 6061-T4

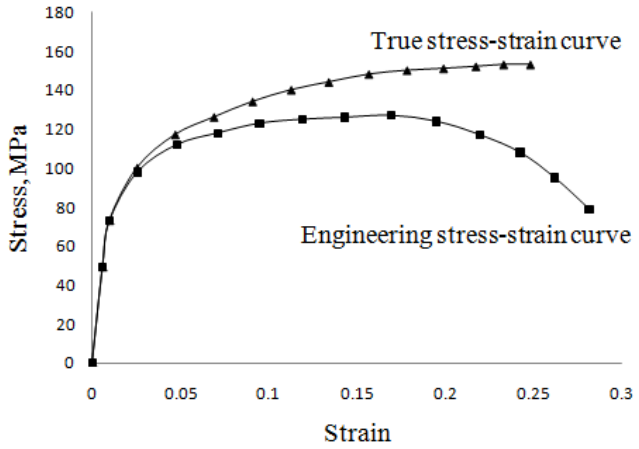

Figure 5. Engineering and true stress-strain curve for AA 6061-O

The strain hardening exponent (n) and the strength coefficient (k) values were summarized in Table 3. It shows that the (n) value for the O-condition more than of the T4-condition, followed by the T651-condition, while the (k) value for O-condition was less than the other conditions, this means the high movement dislocation that produced from internal strain about precipitation atoms was occurred, and provide more grain boundaries to prevent crack propagation in T4 and T651 conditions (Haji, 2010).

Table 3. Values of k and n for three conditions

	n	K (MPa)
AA 6061-T651	0.052	480
AA 6061-T4	0.069	400
AA 6061-O	0.158	110

3.1 Low Cycle Fatigue of Aluminum Alloy AA 6061

Figures 6-8 depict the total strain amplitude versus life in reversals (2N) for alloy AA 6061 at T651, T4 and O-condition respectively. In general, low cycle fatigue life is sensitive to strain amplitude, and the fatigue life decreases as the strain amplitude increases (Fenga, Qiua, Feia, Shana, & Huab, 2010).

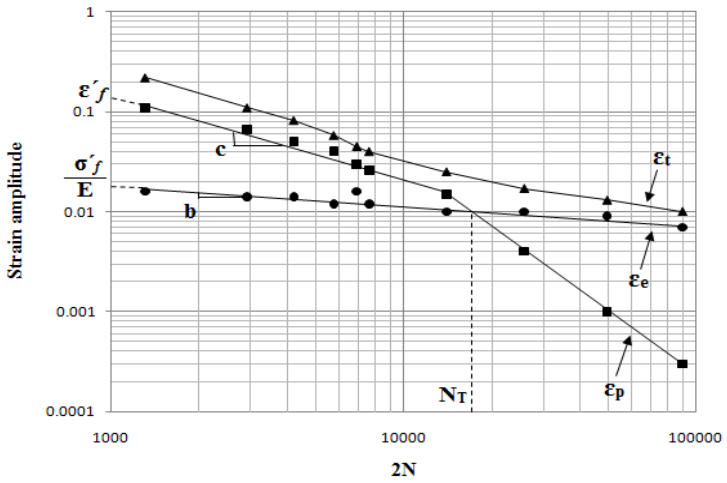

Figure 6. Fatigue life curve for AA 6061-T651

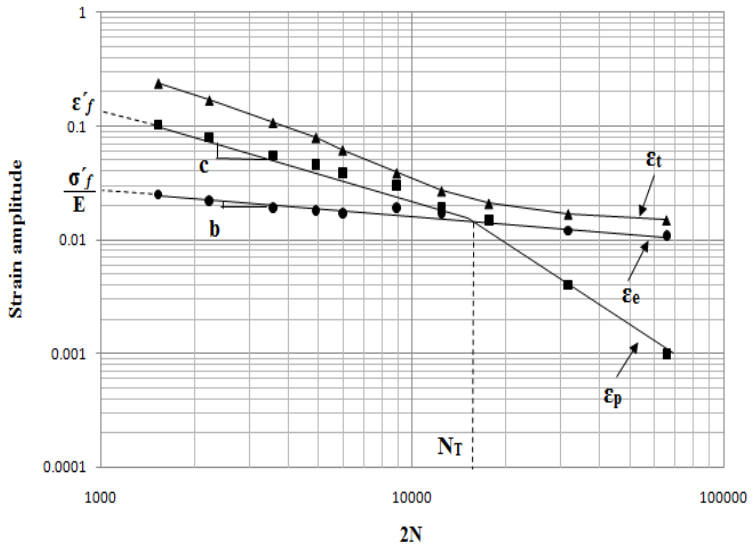

Figure 7. Fatigue life curve for AA 6061-T4

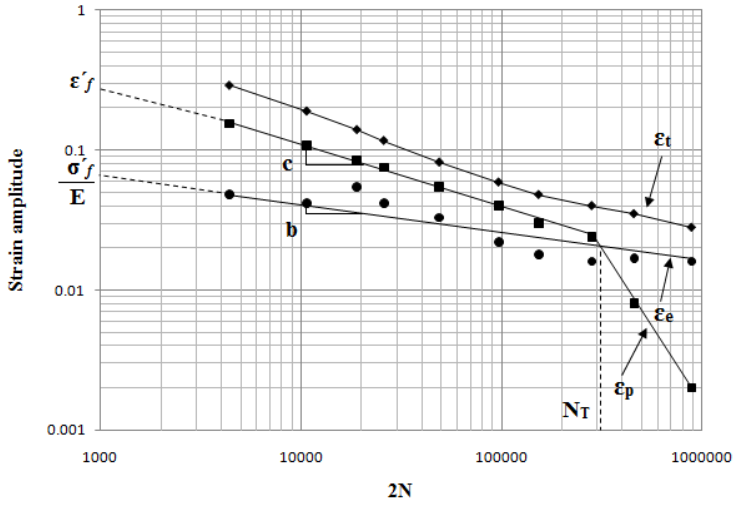

Figure 8. Fatigue life curve for AA 6061-O

The plastic strain component did not reflect the linearity of Coffin-Manson relationship. This plastic strain level is alloy dependent and below critical level there is a departure from single slope behavior. Therefore, in the lower plastic strain region, the Coffin-Manson relationship does not obey the single slope behavior. This deviation from single slope behavior is related to the relative inability of the microstructure to develop homogeneous slip during low plastic strain cycling. This behavior was known as Bi-Linear. Fatemi et al. (2005) attributed the cause of this bi-linearity to the somewhat flat nature of the cyclic stress-strain curve in the inelastic region of these Al alloys. Ignoring the non-linearity can result in large data scatter leading to significant inaccuracies in life predictions.

Fatigue parameters were summarized in Table 4. AA6061-t651 has the highest σ'_f and b values, and lowest ε_f' and c values among other conditions. It can be concluded that the alloy with higher σ'_f and b has higher strength, whereas the alloy with higher ε'_f and c has higher ductility (Basan, Franulovic, Prebil, & Crnjaric-Zic, 2011; Schweizer, Seifert, Nieweg, Hartrott, & Riedel, 2011). Also it can be seen there is no a large differences in most fatigue properties when compared the T651 with T4 conditions, but this difference become very clear as compared these two conditions (T651 and T4) with the O-condition. This convergence and divergence was agreed with tensile properties. The transition life (NT) is defined as the life where the total strain amplitude consists of equal elastic and plastic components, this imply, the life at which the elastic and plastic curves

intersect (Haji, 2010; Borrego et al., 2004; Fenga et al. 2010). The transition life was found to be the highest for O-condition, because it is being the less hardening behavior among other conditions.

Table 4. Low cycle fatigue parameters for aluminum alloy AA6061 at different conditions

	σ'_f	b	ε'_f	c	n'	K' (MPa)	N_T
AA 6061-T651	371	-0.122	0.14	-0.509	0.239	595	16 240
AA 6061-T4	332	-0.120	0.15	-0.520	0.230	514	16 820
AA 6061-O	310	-0.105	0.27	-0.531	0.197	401	310 560

Also it is found that the value of n' for T651 is the highest of the other values. However, it can be observed that the values of n' is close to its monotonic strain hardening values. The variation of cyclic strain hardening exponent is small. This is an evidence of cyclic hardening (Berkovits, 2003).

Since a larger value of "b" produces a more negative slope fatigue life plot, it is clear that a material with high cyclic strain-hardening coefficient is not useful for high cycle fatigue compared with one having low value of n'. On other hand, n' is usually of minor importance compared with σ_f' in defining high cycle fatigue life (Bannantine, Comer, & Handrok, 1989) Thus for design against low cycle fatigue it is desirable to have material that manifest both high ductility and high strength (Crane & Charles, 1987; Bannantine et. al., 1989).

3.2 SEM Examination

Figure 9a, b, and c show SEM examination for specimens at strain closer to true tensile stress (σ_u). There are many crack origins due to high stresses that accompany LCF. In cyclic loading, large single ''craters" (due to particle embedding) appear close to or directly at the edge of the fracture surface. This is a strong indicator for failure originating from the surface (Khan, Vyshnevskyy, & Mosler, 2010). There are three zones which can be identified. The first zone represents the crack origins zone. In this zone, cracks initiated from the surface of the specimen then spread relatively slowly for O-condition (Figure 9c) followed by T4 and T651-conditions respectively (Figure 9b and a). The crack initiation zone has a smooth appearance owing to the rubbing action as cracks propagate through the tested section. The second zone represents the crack propagation with less smooth appearance. This designates that cracks extended more rapidly in this zone. The third zone is the area wherein the final fast fracture zone when the net section became too small to support the applied load and the specimen fractured at this reduced area. The fast fracture zone for T651-condition is large as compared with T4 and O-conditions this related to high strength of T651.

Fatigue fractures exhibited relatively smooth areas for three conditions containing distinct periodic markings generally referred as striations. These rows of parallel markings are the result of a particle (or set of particles) on one fatigue fracture surface being successively impressed into the surface of the mating half of the fracture during the closing portion of the fatigue cycle.

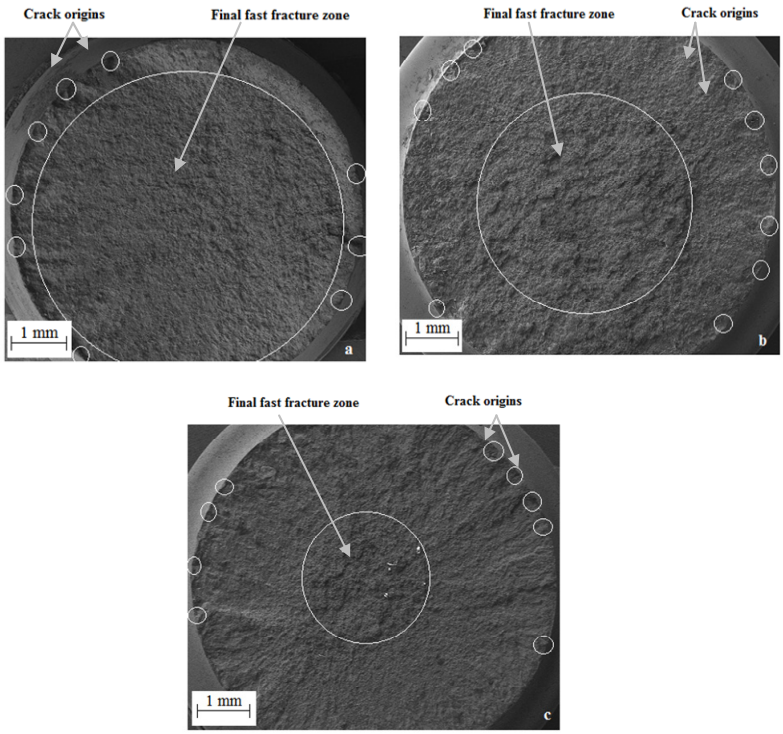

Figure 9. SEM of fracture feature of AA 6061 at σ_u a) T651 b) T4 and c) O-condition

Figure 10 shows that the fracture surface contained ductile striation. Striations formed during crack propagation stage. Large second-phase particles and inclusions in 6061 aluminum alloy can change the local crack growth rate resulting in fatigue striation spacing (Marini et al., 2011). The clearness of fatigue striations which give an indication about the orientation of the crack propagation (Ovono, Guillot, & Massinon, 2008). This striations were very clear for O-condition (Figure 10c) as compared with the other two conditions (Figure 10a and b) because there is high plastic deformation. Secondary crack also appeared in different regions that may be congregate in some points in addition to small voids were dispersed.

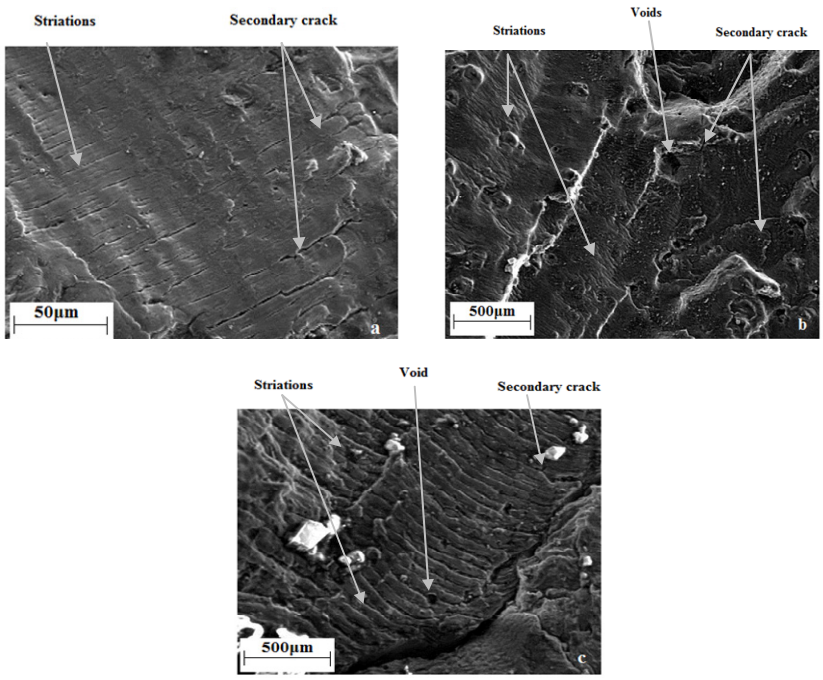

Figure 10. SEM images show striations for a) T651 b) T4 and c) O-conditions

Figure 11 shows shear dimples fracture surface resulting from fatigue loading. This fracture surface describes ductile fracture that formed through a process which called void coalescence. Slip is the cause of plastic deformation of material that occurred between the voids (Marini et al., 2011). Also it can be found a large number of dimples with different sizes for T4 and T651 conditions.

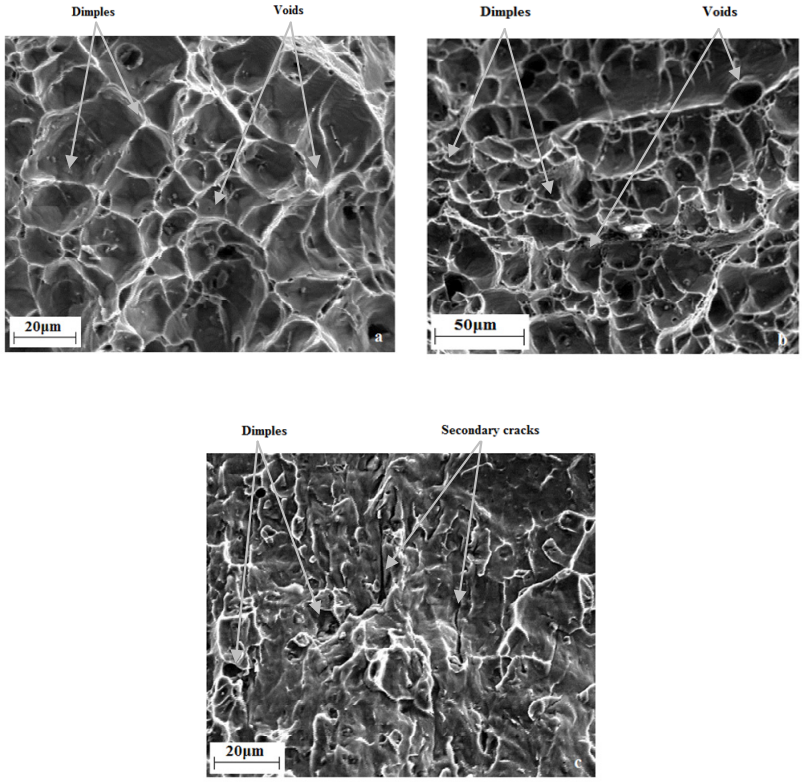

Figure 11. SEM images show dimples for a) T651, b) T4 and c) O-conditions

4. Conclusions

1) The LCF behavior of AA6061-O, T4 and T651 can be predicted using strain hardening exponent, n, or σ_u/σ_y ratio.
2) The values of fatigue ductility exponent (b) and fatigue strength exponent (c) for three conditions (annealing, T4 and T651) are within the values of metallic materials.
3) AA6061-O has the larger vale of $\square_f'$, so the annealed condition has the larger hardening behavior than the other two conditions.
4) The highest value of N_T is for O-condition followed by T4 and T651.
5) The highest value of cyclic hardening exponent, n', was recorded in T651 condition followed by T4 and the lowest was in O-condition.
6) The striations were very clear for O-condition due to higher plastic deformation.

Acknowledgements

We would like to express our sincere gratitude to my friends working in Technical College-Baghdad for continuously supporting us in this research, and also for their patience, motivation, enthusiasm, and immense knowledge. Their guidance has helped us during the time of research and writing it.

References

Bannantine, J., Comer, J., & Handrok, J. (1989). *Fundamentals of metal fatigue analysis*. New Jersey, 07632: Prentice Hall, Englewood Cliffs.

Basan, R., Franulovic, M., Prebil, I., & Crnjaric-Zic, N. (2011). Analysis of strain-life fatigue parameters and behavior of different groups of metallic materials. *International Journal of Fatigue, 33*, 484-491. http://dx.doi.org/10.1016/j.ijfatigue.2010.10.005

Berkovits, A. (2003). Variation of the cyclic strain hardening exponent in advanced aluminum alloys. *International Journal of Fatigue, 9*(4), 229-232.

Borrego, L. P., Abreu, L. M., Costa, J. M., & Ferreira, J. M. (2004). Analysis of low cycle fatigue in AlMgSi aluminum alloys. *Engineering Failure Analysis, 11*, 715-725. http://dx.doi.org/10.1016/j.engfailanal.2003.09.003

Crane, F., & Charles, J. (1987). Selection and use of engineering materials (2nd ed.). *Adlard & Sons, UK*.

Ding, H. Z., Biermann, H., & Hartmann, O. (2002). A low cycle fatigue model of a short-fibre reinforced 6061 aluminum alloy metal matrix composite. *Composites Science and Technology, 62*, 2189-2199. http://dx.doi.org/S0266-3538 (02)00160-4

Ding, H. Z., H. Biermann, H., Hartmann, O., & Mughrabi, H. (2002). Modeling low-cycle fatigue life of particulate-reinforced metal-matrix composites. *Materials Science and Engineering, A333*, 295-305. http://dx.doi.org/S0921-5093 (01)01854-8

Fatemia, A., Plaseieda, A., Khosrovanehb, A. K., & Tanner, D. (2005). Application of bi-linear log–log S–N model to strain-controlled fatigue data of aluminum alloys and its effect on life predictions. *International Journal of Fatigue, 27*, 1040-1050. http://dx.doi.org/10.1016/j.ijfatigue.2005.03.003

Fenga, M. D., Qiua, H. G., Feia, H. Z., Shana, L. X., & Huab, Z. W. (2010). Effect of microstructural features on fatigue behavior in A319-T6 aluminum alloy. *Materials Science and Engineering, 527*, 3420-3426. http://dx.doi.org/10.1016/j.msea.2010.02.055

Haji, Z. N. (2010). Low cycle fatigue behavior of aluminum alloys AA2024-T6 and AA7020-T6. *Diyala Journal of Engineering Sciences* (pp. 127-137). http://dx.doi.org/S2408_P0369

Khan, S., Vyshnevskyy, A., & Mosler, J. (2010). Low Cycle Life Time Assessment of Al 2024 Alloy. *International Journal of Fatigue, 32*, 1270-1277. http://dx.doi.org/10.1016/j.ijfatigue.2010.01.014

Kwon, S., Song, K., Shin, K. S., & Kwun, S. I. (2010). Low cycle fatigue properties and cyclic deformation behavior of as-extruded AZ31 magnesium alloy. *Trans. Nonferrous Met. Soc., 20*, 533-539. Retrieved from http://www.tnmsc.cn

Liu, X, S., He, G. Q., Ding, X. Q., Mo, D. F., & Zhang, W. H. (2009). Fatigue behavior and dislocation substructures for 6063 aluminum alloy under nonproportional loadings. *International Journal of Fatigue, 31*, 1190-1195. http://dx.doi.org/10.1016/j.ijfatigue.2008.11.019

Marini, M., & Ismail, A. B. (2011). Torsional deformation and fatigue behavior of 6061 aluminum alloy. *IIUM Engineering Journal, 12*(6), Special Issue in Science and Ethics.

Mustapha, B., Abdelhamid, H., & Mohamed, B. (2009). Heat treatment effect on fatigue crack growth. *International Conference on Integrity, Reliability and Failure,* 3. Retrieved from http://Porto/Portugal/S2408_P0369

Ovono, D., Guillot, I., & Massinon, D. (2008). Study on low cycle fatigue behavior of the aluminum cast alloys. *Journal of Alloys and Compounds, 52*, 425-431.

Schweizer, C., Seifert, T., Nieweg, B., Hartrott, P., & Riedel, H. (2011). Mechanisms and modeling of fatigue crack growth under combined low and high cycle fatigue loading. *International Journal of Fatigue,* 33, 194-202.

Snchez-Santana, U., Rubio-Gonzlez, C., Mesmacque, G., & Amrouche, A. (2009*).* Effect of fatigue damage on the dynamic tensile behavior of 6061-T6 aluminum alloy and AISI 4140T steel. *International Journal of Fatigue, 31*, 1928-1937.

Xue, L. (2008). A unified expression for low cycle fatigue and extremely low cycle fatigue and its implication for monotonic loading. *International Journal of Fatigue, 30*, 1691-1698. http://dx.doi.org/10.1016/j.ijfatigue.2008.03.004